



Brief paper

Enclosing a target by nonholonomic mobile robots with bearing-only measurements[☆]Ronghao Zheng^a, Yunhui Liu^b, Dong Sun^a^a Department of Mechanical and Biomedical Engineering, City University of Hong Kong, 83 Tat Chee Avenue, Kowloon, Hong Kong, China^b Department of Mechanical and Automation Engineering, The Chinese University of Hong Kong, Hong Kong, China

ARTICLE INFO

Article history:

Received 22 May 2014

Received in revised form

15 December 2014

Accepted 23 December 2014

Available online 11 February 2015

Keywords:

Distributed robot systems

Multiple mobile robots

Surveillance systems

Wheeled robots

ABSTRACT

This paper addresses the problem of steering a single or a group of autonomous nonholonomic mobile robots to enclose a target of interest. We develop control schemes which require only local bearing measurements, and deal with encirclement of two types of targets: point target and disk target. When a single robot is used, circumnavigation schemes are proposed to achieve effective encirclement of the target. It is shown that under the proposed control schemes, the robot can circle the target from a prescribed distance without distance measurement. When multiple robots are deployed, the control schemes developed for single robot are modified by introducing a coordination mechanism, which drives the robots to distribute evenly around the target. We further discuss a control scheme that moves the robots to form a static circular formation around the target based on feedback linearization. All the proposed control schemes are validated in experiments on a group of two-wheeled differential drive mobile robots.

© 2015 Elsevier Ltd. All rights reserved.

1. Introduction

Enclosing a target or an area of interest represents a promising application of mobile robots in many areas such as security and surveillance, search and rescue, orbit maintenance, and source localization. Autonomous mobile robots, either a single robot or a group of robots, can be deployed to perform such tasks (Feddema, Lewis, & Schoenwald, 2002). Enclosing a target by holonomic mobile robots was reported in the literature, such as (Guo, Yan, & Lin, 2010; Kim & Sugie, 2007; Yamaguchi, 1999). Nonholonomic mobile robots, although their control is much more challenging, were also studied in some works, for example Ceccarelli, Di Marco, Garulli, and Giannitrapani (2008), Lan, Yan, and Lin (2010) and Zheng, Lin, Fu, and Sun (2013). Some commercial products, such as the Kestrel autopilot system, also provide target monitoring function for unmanned aerial vehicles.

In most of these existing works, it is commonly assumed that measurements of relative positions amongst the robots are available, which, however, restricts many practical applications. For example, for a mobile robot equipped with single omnidirectional camera, or underwater vehicle equipped with radar and sonar operating in passive listening mode, it is difficult or even impossible to obtain the distance measurement. Motivated by these potential applications, formation control utilizing bearing-only measurements has attracted a lot of attention recently. In bearing-based formation control, it is assumed that the robots can only measure the local bearings of their surrounding objects. Compared with relative position sensors or distance sensors, bearing-only sensors are simpler and cheaper but still span a large spectrum of common sensor types such as monocular camera systems. Some works on single robot target enclosing using bearing measurements have been reported. For example, a circumnavigation strategy was proposed for holonomic robot in Deghat, Shames, Anderson, and Yu (2010) and was extended to nonholonomic robot in Deghat et al. (2012). In Deghat et al. (2012) and Deghat et al. (2010), a nonlinear periodically time-varying algorithm was used to estimate the position of the target. The control algorithm was then built based on the estimated position. However, this method assumes that the robot knows its own position in an inertial coordinate frame.

The problem of enclosing a target with multiple robots using bearing-only measurements has been rarely studied. Guo, Yan, and Lin (2011) proposed a bearing-only control strategy with inter-agent gossip communication to drive a group of robots to achieve

[☆] The work of Zheng is supported through the Hong Kong Ph.D. Fellowship Scheme. The work was also supported in part by a grant from Research Grants Council of the Hong Kong Special Administrative Region, China (Reference No. CUHK6/CRF/13G assigned to CityU). The material in this paper was not presented at any conference. This paper was recommended for publication in revised form by Associate Editor Warren E. Dixon under the direction of Editor Andrew R. Teel.

E-mail addresses: rzheng3-c@my.cityu.edu.hk (R. Zheng), yhliu@mae.cuhk.edu.hk (Y. Liu), medsun@cityu.edu.hk (D. Sun).

and maintain a balanced circular formation around a target. Bearing-based control strategies have been studied to solve some other problems in multirobot systems. For example, Moshtaghi, Michael, Jadbabaie, and Daniilidis (2009) designed a control law based on the bearing angle, the optical flow and time to collision for a group of constant-speed nonholonomic robots to achieve parallel and circular formations. Bearing-only triangular formation control of three mobile agents was considered in Basiri, Bishop, and Jensfelt (2010), in which each agent used locally measured bearings to establish and maintain a pre-specified angular separation relative to the other two agents. The controller in Basiri et al. (2010) was relaxed in Bishop (2011a). For both papers, the proof of global stability is based on Poincaré-Bendixson theorem and thus the number of agents is limited. Quadrilateral formation control using similar controllers, given in Bishop (2011b), was proved using Lyapunov based method. It would be of great interest to generalize the formulation to arbitrary number of agents, which still remains unsolved. Zhao, Lin, Peng, Chen, and Lee (2013) proved the local finite-time stability of angle-constraint cyclic formation with arbitrary number of holonomic agents under a discontinuous control law. The rendezvous problem of nonholonomic robots using bearing-only control strategies was studied in Zheng and Sun (2013a) and was experimentally tested in Zheng and Sun (2013b).

In addition, direction-constraint formation control was studied by Bishop, Shames, and Anderson (2011). Eren (2012) and Franchi et al. (2012) studied bearing-constraint formation control for non-holonomic robots. It is worth noting that unlike bearing-based formation control, both direction-constraint and bearing-constraint formations only require the desired geometrical relationships to be specified in terms of relative angular constraints between agent-pairs, which implies that the distance measurement may be still needed while implementing the controllers.

In this paper, we investigate the bearing-based target enclosing problem using single robot and multiple robots, respectively. The proposed control schemes are validated by means of real experiments employing a team of mobile robots. Our main contributions in this paper are twofold. First, we develop novel control schemes for nonholonomic mobile robots to enclose a target with relative bearing measurements only. Unlike Deghat et al. (2012, 2010), we assume that global position information is not available and the robots are memoryless so they cannot know their own positions in any inertial coordinate frame. Unlike Guo et al. (2011), we assume that there is no inter-agent communication so that the robots cannot share their bearing measurements amongst each other. Hence, the proposed controller schemes are simple and can be easily implemented on real robots. Second, collision avoidance between the robot and disk-area target is guaranteed with our control schemes. Inter-agent collision avoidance is also considered by exploiting a simple behavior-based algorithm.

The rest of the paper is organized as follows. Section 2 presents our control schemes to achieve circumnavigation using a single robot while Section 3 discusses the distributed circumnavigation and balanced circular formation by using multiple robots. In Section 4, we present experimental results to demonstrate the effectiveness of the proposed control schemes. Finally, we draw conclusions and suggest future research directions in Section 5.

2. Enclosing a target by single robot

Consider a nonholonomic, two-wheeled differential drive robot moving in a 2D workspace. The kinematic equation of each robot can be written as

$$\dot{x} = v \cos \theta, \quad \dot{y} = v \sin \theta, \quad \dot{\theta} = \omega, \quad (1)$$

where $(x, y) \in \mathbb{R}^2$ is the location of the robot and θ the heading angle with respect to a global coordinate frame $^g \Sigma$. Control input

$v \in [-v_{\max}, v_{\max}]$ is the forward speed in the direction of θ , and another control input $\omega \in [-\omega_{\max}, \omega_{\max}]$ is the angular speed. Here v_{\max} and ω_{\max} (both positive) are the bounds for forward and angular speeds, respectively.

Consider a static target \mathcal{T} centered at (x_b, y_b) in the plane, which can be either a point or a disk area. To accomplish the mission, the robot equips an onboard sensor. However, this sensor only allows the robot to detect the bearing information of its surrounding objects, i.e., distance information is not available. It is also assumed that the target can be always detected by the sensor.

When there is only one single robot, a possible way to efficiently surveil or protect the target is to let the robot circle around the target at a stand-off distance. Following works such as Cao, Muse, Casbeer, and Kingston (2013), Shames, Dasgupta, Fidan, and Anderson (2012) and Tang, Shinzaki, Gage, and Clark (2012), we call it *circumnavigation*. To facilitate the analysis, we define

$$\rho := \sqrt{(x - x_b)^2 + (y - y_b)^2}, \quad \alpha := \arctan2(\tilde{y}_b, \tilde{x}_b), \quad (2)$$

where $\arctan2(y, x)$ represents a two-argument arctangent function retuning the angle of point (x, y) as a numeric value between $-\pi$ and π radians. And $(\tilde{x}_b, \tilde{y}_b)$ is that Cartesian coordinates of the target \mathcal{T} in the robot's local frame $^r \Sigma$, i.e.,

$$\begin{bmatrix} \tilde{x}_b \\ \tilde{y}_b \end{bmatrix} = \begin{bmatrix} \cos \theta & \sin \theta \\ -\sin \theta & \cos \theta \end{bmatrix} \begin{bmatrix} x_b - x \\ y_b - y \end{bmatrix}.$$

In our setting, only α is measurable. Because ρ cannot be measured, the relative position $(\tilde{x}_b, \tilde{y}_b)$ is unavailable. After straightforward calculation, the dynamics of ρ and α can be described as

$$\dot{\rho} = -v \cos \alpha, \quad \dot{\alpha} = -\omega + v \sin \alpha / \rho, \quad (3)$$

where $(\rho, \alpha) \in (0, \infty) \times [-\pi, \pi)$.

2.1. Controller 1: single robot enclosing a point target

We first consider the case of enclosing a point target by a single robot. The following control law is proposed and analyzed:

Controller 1:

$$\begin{cases} v = k_v v_{\max} \cos(\alpha + \varphi), \\ \omega = k_\omega \omega_{\max} \sin(\alpha + \varphi), \end{cases} \quad (4)$$

where $k_v, k_\omega \in (0, 1]$ are control gains for forward speed and angular speed, respectively. The following theorem shows that the desired circling behavior can be achieved by setting

$$\varphi = -\arctan \frac{\rho^* k_\omega \omega_{\max}}{k_v v_{\max}}, \quad (5)$$

where ρ^* is the predefined stand-off distance.

Theorem 1. Under the controller 1 with (5), a robot described by (1) will eventually move on a circle centered at (x_b, y_b) with radius ρ^* counter-clockwise at speed $k_v v_{\max} \sin(-\varphi)$.

Proof. First of all, it is clear that under controller 1, $v \in [-v_{\max}, v_{\max}]$ and $\omega \in [-\omega_{\max}, \omega_{\max}]$. Consider the following point

$$\begin{bmatrix} x_c \\ y_c \end{bmatrix} := \begin{bmatrix} x \\ y \end{bmatrix} + \rho^* \begin{bmatrix} -\sin \theta \\ \cos \theta \end{bmatrix}, \quad (6)$$

we can see that (x_c, y_c) is the center when the robot performs counter-clock uniform circular motion on a circle of radius ρ^* . We will show that $(x_c, y_c) \rightarrow (x_b, y_b)$ as $t \rightarrow \infty$.

The derivative of (x_c, y_c) with respect to time can be calculated as

$$\begin{bmatrix} \dot{x}_c \\ \dot{y}_c \end{bmatrix} = \begin{bmatrix} \cos \theta \\ \sin \theta \end{bmatrix} (v - \rho^* \omega).$$

Under (4) and (5), we have

$$\begin{aligned} v - \rho^* \omega &= k_v v_{\max} \cos(\alpha + \varphi) - \rho^* k_w \omega_{\max} \sin(\alpha + \varphi) \\ &= k_1 [\cos(-\varphi) \cos(\alpha + \varphi) - \sin(-\varphi) \sin(\alpha + \varphi)] = k_1 \cos \alpha, \end{aligned}$$

where we define $k_1 := \sqrt{(k_v v_{\max})^2 + (\rho^* k_w \omega_{\max})^2}$ for brevity. Furthermore,

$$\begin{aligned} \cos \alpha &= [\cos \theta (x_b - x) + \sin \theta (y_b - y)] / \rho \\ &\stackrel{(6)}{=} [\cos \theta (x_b - x_c) + \sin \theta (y_b - y_c)] / \rho. \end{aligned} \quad (7)$$

Consider the following Lyapunov function candidate,

$$V = \frac{1}{2} [(x_c - x_b)^2 + (y_c - y_b)^2], \quad (8)$$

whose derivative is

$$\dot{V} = -\frac{k_1}{\rho} [\cos \theta (x_c - x_b) + \sin \theta (y_c - y_b)]^2 \leq 0.$$

It can be seen that $\dot{V} = 0$ only when

$$\cos \theta (x_c - x_b) + \sin \theta (y_c - y_b) = 0, \quad (9)$$

i.e., $\cos \alpha = 0$ according to (7).

We next show that the largest invariance set in $\{(x_c, y_c) | \dot{V} = 0\}$ is $\{(x_b, y_b)\}$. When $\cos \theta (x_c - x_b) + \sin \theta (y_c - y_b) = 0$, $(\dot{x}_c, \dot{y}_c) = (0, 0)$, we then have

$$\begin{aligned} \frac{d}{dt} [\cos \theta (x_c - x_b) + \sin \theta (y_c - y_b)] \\ = \omega [-\sin \theta (x_c - x_b) + \cos \theta (y_c - y_b)]. \end{aligned}$$

When $\cos \alpha = 0$, $\omega = k_w \omega_{\max} \sin(\pm \pi/2 + \varphi) \neq 0$. To satisfy $\cos \theta (x_c - x_b) + \sin \theta (y_c - y_b) \equiv 0$, it requires that

$$-\sin \theta (x_c - x_b) + \cos \theta (y_c - y_b) = 0. \quad (10)$$

Combining both (9) and (10), we get

$$\underbrace{\begin{bmatrix} \cos \theta & \sin \theta \\ -\sin \theta & \cos \theta \end{bmatrix}}_A \begin{bmatrix} x_c - x_b \\ y_c - y_b \end{bmatrix} = \begin{bmatrix} 0 \\ 0 \end{bmatrix}.$$

Since matrix A is full rank, the largest invariance set in $\{(x_c, y_c) | \dot{V} = 0\}$ is $\{(x_b, y_b)\}$. Then according to LaSalle's invariance theorem (Khalil, 2002, Theorem 4.4), the trajectory of (x_c, y_c) converges to (x_b, y_b) , i.e., the trajectory of (x, y) converges to a circle centered at (x_b, y_b) with radius ρ^* . The eventual speed of the robot can be calculated accordingly. \square

2.2. Controller 2: single robot with fixed forward speed enclosing a point target

For some kinds of mobile vehicles, such as those considered in Deghat et al. (2012) and Matveev, Hoy, and Savkin (2013), the forward speed v is fixed and requires $v \geq v_{\min} > 0$. This requirement motivates us to propose the following control law:

Controller 2:

$$\begin{cases} v = \min(k_v v_{\max}, \eta k_w \omega_{\max} \rho^*), \\ \omega = v / \rho^* - (1 - \eta) k_w \omega_{\max} \cos \alpha, \end{cases} \quad (11)$$

where control gains $k_v, k_w \in (0, 1]$ and $\eta \in (0, 1)$ is a design parameter which can be used to adjust the forward speed.

Theorem 2. Given $\bar{v} = \min(k_v v_{\max}, \eta k_w \omega_{\max} \rho^*) \geq v_{\min}$, under controller 2, a robot described by (1) with constant forward velocity \bar{v} will eventually move on circle centered at (x_b, y_b) with radius ρ^* counter-clockwise.

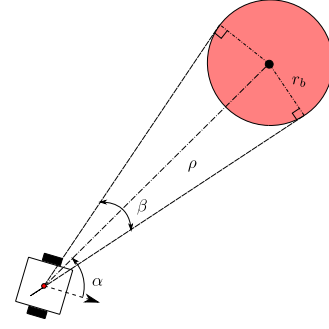


Fig. 1. An illustration of defined variables. The disk represents the target.

Proof. Clearly, $v \in [v_{\min}, v_{\max}]$. For ω , one has $\omega \leq \eta k_w \omega_{\max} + (1 - \eta) k_w \omega_{\max} \leq \omega_{\max}$ and $\omega \geq v_{\min} / \rho^* - (1 - \eta) k_w \omega_{\max} \geq -k_w \omega_{\max}$, so $\omega \in [-\omega_{\max}, \omega_{\max}]$.

Under controller 2, we obtain the following equation based on (6):

$$\begin{bmatrix} \dot{x}_c \\ \dot{y}_c \end{bmatrix} = \begin{bmatrix} \cos \theta \\ \sin \theta \end{bmatrix} (v - \rho^* \omega) = k_1 \begin{bmatrix} \cos \theta \\ \sin \theta \end{bmatrix} \begin{bmatrix} \cos \theta \\ \sin \theta \end{bmatrix}^T \begin{bmatrix} x_b - x_c \\ y_b - y_c \end{bmatrix},$$

where we define $k_1 := (1 - \eta) k_w \omega_{\max} \rho^* / \rho$ for brevity. Consider the Lyapunov function candidate (8), it is obtained that

$$\dot{V} = -k_1 [\cos \theta (x_c - x_b) + \sin \theta (y_c - y_b)]^2 \leq 0.$$

The following argumentation is similar to that of Theorem 1 and is omitted here. \square

2.3. Controller 3: single robot enclosing a disk target with guaranteed collision avoidance

In this subsection, we consider the case when the target is a disk area (see Fig. 1). Let r_b be the radius of the target disk. Because the onboard sensor can only provide bearing measurement, r_b is unavailable to the robot. However, unlike the case of enclosing a point target, collision avoidance between the robot and the disk target must be taken into account, i.e., it should be guaranteed that $\rho(t) > r_b$ for all $t \geq 0$. To do that, we utilize the measured subtended angle $\beta \in (0, \pi)$ (see Fig. 1).

The proposed control law is given by

Controller 3:

$$\begin{cases} v = \bar{v} \cos(\alpha + \varphi), \\ \omega = v / \rho^* - (1 - \eta) k_w \omega_{\max} \cos \alpha, \end{cases} \quad (12)$$

where $\bar{v} := \min(k_v v_{\max}, \eta k_w \omega_{\max} \rho^*)$, $\eta \in (0, 1)$ is a design parameter. Moreover, the offset angle φ is designed to be

$$\varphi = -\mu\pi - (1 - \mu)\pi \exp[k_\beta(\beta - \beta_{\max})] \quad (13)$$

with $\mu \in (0, 1)$, $k_\beta > 0$, and $\beta_{\max} \in (0, \pi)$ is the maximum allowed subtended angle. The value of μ affects the convergence rate significantly. For example, if μ is too small (≈ 0), then the eventual forward speed around the target may also be too small; If μ is too large (≈ 1) and it happens that $\cos \alpha \approx 0$, then the robot will approach the target very slowly when it is far away from the target disk.

We first show in the following theorem that under controller 3, a robot can avoid collision with the target disk.

Theorem 3. Under controller 3 with (13), if $\beta(0) < \beta_{\max}$,¹ then $\rho(t) > r_b$ for all $t \geq 0$.

¹ That is, $\rho(0) > r_b \csc \frac{\beta_{\max}}{2}$.

Proof. Under controller 3, from (3) one obtains

$$\dot{\rho} = -\bar{v} \cos(\alpha + \varphi) \cos \alpha.$$

As $\rho \rightarrow (r_b \csc \frac{\beta_{\max}}{2})^+$, $\beta \rightarrow (\beta_{\max})^-$, so $\varphi \rightarrow -\pi$ according to (13). As a result, we have $\dot{\rho} \rightarrow \bar{v} \cos^2 \alpha \geq 0$. Therefore $\rho(t) > r_b \csc \frac{\beta_{\max}}{2} > r_b$ for all $t \geq 0$. \square

The following theorem shows that a robot can achieve circumnavigation around the target disk using the proposed control law.

Theorem 4. Under controller 3 with (13), if $\beta_{\max} > 2 \arcsin \frac{r_b}{\rho^*}$ and $\rho(0) > r_b \csc(\beta_{\max}/2)$, then a robot described by (1) will eventually move on a circle centered at (x_b, y_b) with radius ρ^* at speed

$$\bar{v} \sin\{\mu\pi + (1 - \mu)\pi \exp[k_\beta(\beta^* - \beta_{\max})]\}$$

with $\beta^* = 2 \arcsin(r_b/\rho^*)$.

Proof. The proof is similar to that of Theorems 1 and 2 and is omitted here. \square

Under controllers 1 and 2, it would cause no problem when the initial position of the robot is close to the target. However, the controller 3 requires that the initial distance from the robot to the center of the target disk $\rho(0) \geq r_b \csc \frac{\beta_{\max}}{2}$. Otherwise, collision may happen.

3. Enclosing a target by multiple robots

In this section, we deal with the case that multiple robots enclose a target. Consider a group of n (≥ 3) mobile robots described by

$$\dot{x}_i = v_i \cos \theta_i, \quad \dot{y}_i = v_i \sin \theta_i, \quad \dot{\theta}_i = \omega_i, \quad (14)$$

where $i = 1, 2, \dots, n$. For multirobot case, we require that the robots not only converge to the desired stand-off circle but also form an optimal configuration. In the target enclosing problem, an optimal configuration often corresponds to an equiangular spaced formation around the target (Bishop, Fidan, Anderson, Doğançay, & Pathirana, 2010). We also require the control schemes to be distributed which allow the team to be robust to insertion and deletion of team members.

3.1. Controller 4: multiple robots enclosing a point target

In this subsection, we modify the control schemes proposed in Section 2 to work in a multirobot scenario.

Let ρ_i and α_i be defined as ρ and α in (2) by replacing (x, y, θ) with (x_i, y_i, θ_i) . To be more practical, it is assumed that the robots cannot detect each other until their distance is smaller than a threshold distance r_s . We denote the neighbor set of robot i as $\mathcal{N}_i = \{j | \sqrt{(x_j - x_i)^2 + (y_j - y_i)^2} \leq r_s, j \neq i\}$. The bearing angle of robot j in robot i 's local frame can be defined formally as $\alpha_j^i = \arctan2(y_j^i, x_j^i)$, $j \in \mathcal{N}_i$, where (x_j^i, y_j^i) is the relative position of robot j in robot i 's local frame, i.e.,

$$\begin{bmatrix} x_j^i \\ y_j^i \end{bmatrix} = \begin{bmatrix} \cos \theta_i & \sin \theta_i \\ -\sin \theta_i & \cos \theta_i \end{bmatrix} \begin{bmatrix} x_j - x_i \\ y_j - y_i \end{bmatrix}.$$

As mentioned before, (x_j^i, y_j^i) is unmeasurable and only α_j^i is measurable. For convenience of presentation, we also define

$$\sigma_+^i = \begin{cases} \min(\alpha_j^i), & \text{if } \mathcal{N}_+^i \neq \emptyset, \\ \pi/2, & \text{if } \mathcal{N}_+^i = \emptyset, \end{cases} \quad (15)$$

and

$$\sigma_-^i = \begin{cases} \pi - \max(\alpha_j^i), & \text{if } \mathcal{N}_-^i \neq \emptyset, \\ \pi/2, & \text{if } \mathcal{N}_-^i = \emptyset, \end{cases} \quad (16)$$

where $\mathcal{N}_+^i = \{j \in \mathcal{N}_i | \alpha_j^i \in (0, \pi/2)\}$ and $\mathcal{N}_-^i = \{j \in \mathcal{N}_i | \alpha_j^i \in (\pi/2, \pi)\}$.

We then modify the control laws proposed in Section 2 to a multirobot scenario by introducing a new control coefficient and defining new control inputs (v_i', ω_i') as

Controller 4:

$$\begin{cases} v_i' = f(\sigma_+^i/\sigma_-^i) v_i, \\ \omega_i' = f(\sigma_+^i/\sigma_-^i) \omega_i. \end{cases} \quad (17)$$

Here (v_i, ω_i) can be any one of controllers 1, 2 and 3. In order to achieve an even distribution, all the robots use same control gains and parameters. Here

$$f : (0, +\infty] \rightarrow (0, 1] \quad (18)$$

is any strictly increasing continuous function. For example, we can let $f(x) = 1 - \exp(-x)$.

Define ϕ_i to be the bearing of robot i position with respect to the target position: $\phi_i = \arctan2(y_i - y_b, x_i - x_b) \bmod 2\pi$. For the convenience of analysis, we label the robots at time t according to their positions in a counterclockwise radial order around the target, i.e., $j > k \Leftrightarrow \phi_j \geq \phi_k$. We also define $\delta\phi_i = \phi_{i+1} - \phi_i$ for $i \in \{1, \dots, n-1\}$ and define $\delta\phi_n = \phi_1 + 2\pi - \phi_n$. Note that $\delta\phi_i \in [0, 2\pi)$ for all i under this labeling.

Theorem 5. Under controller 4, if $r_s > 2\rho^* \sin(\pi/n)$, the equilibrium point given by $\{\rho_i = \rho^*, \alpha_i = \pi/2, \delta\phi_i = 2\pi/n, \forall i\}$ is (locally) asymptotically stable.

Proof. Based on the analysis in Section 2, because $f(\sigma_+^i/\sigma_-^i) > 0$ for all $t \geq 0$, then for all i , $\rho_i \rightarrow \rho^*$ and $\alpha_i \rightarrow \pi/2$ as $t \rightarrow \infty$.

The condition $r_s \geq 2\rho^* \sin(\pi/n)$ guarantees that neither \mathcal{N}_+^i nor \mathcal{N}_-^i is empty around the equilibrium point. Therefore, when $\rho_i = \rho^*$ and $\alpha_i = \pi/2$ for all i , using simple trigonometry, we have (see Fig. 2)

$$\sigma_+^i = \delta\phi_i/2 \quad \text{and} \quad \sigma_-^i = \delta\phi_{i-1}/2.$$

Around the equilibrium point, it is obtained that

$$\dot{\phi}_i = \omega_i' = f(\delta\phi_i/\delta\phi_{i-1}) \omega^*,$$

where ω^* is the angular velocity when $\rho_i = \rho^*$ and $\alpha_i = \pi/2$. The above equation leads to

$$\frac{d}{dt} \delta\phi_i = [f(\delta\phi_{i+1}/\delta\phi_i) - f(\delta\phi_i/\delta\phi_{i-1})] \omega^*.$$

Define $\bar{M} = \{j | \delta\phi_j = \max \delta\phi_i\}$ and $\underline{M} = \{j | \delta\phi_j = \min \delta\phi_i\}$. When $\bar{M} \neq \underline{M}$, we have

$$\frac{\sum_{j \in \bar{M}} \delta\phi_j}{dt |\bar{M}|} < 0 \quad \text{and} \quad \frac{\sum_{j \in \underline{M}} \delta\phi_j}{dt |\underline{M}|} > 0.$$

So we conclude that the equilibrium point defined by $\{\rho_i = \rho^*, \alpha_i = \pi/2, \delta\phi_i = 2\pi/n, \forall i\}$ is locally asymptotically stable. \square

Given the stand-off distance ρ^* , the equilibrium point in Theorem 5 is fixed. When given different ρ^* , the robots can move on different orbits. However, in that case, an even distribution will not be achieved.

3.2. Controller 5: multiple robots enclosing a disk target

By keeping the robots in motion, controllers 1–4 provide solutions to effectively surveil or protect a target when the number of robots is limited. However, if there are enough robots to achieve a tight enclosing, an alternative way is to drive the robots to form a balanced circular formation around the target. In this way, because

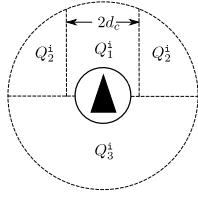


Fig. 4. The partition of Q_1^i , Q_2^i , and Q_3^i when $v_i > 0$.

Similarly, for $j \in \underline{M}$, we have $\varsigma_+^{j+1} \geq \varsigma_-^{j+1} = \varsigma_+^j \leq \varsigma_-^j$. Moreover, when $\underline{M} \neq \overline{M}$, the condition $r_s \geq 2r_b \csc(\beta^*/2) \sin(\pi/n)$ guarantees that there exists at least one $j \in \underline{M}$ with $\varsigma_+^j < \varsigma_-^j$, so

$$\begin{aligned} \frac{d}{dt} \frac{\sum_{j \in \underline{M}} \delta \phi_i}{|\underline{M}|} &= \frac{1}{|\underline{M}|} \sum_{j \in \underline{M}} \left[f(\varsigma_+^{j+1}/\varsigma_-^{j+1}) - f(\varsigma_+^j/\varsigma_-^j) \right] \\ &= \frac{1}{|\underline{M}|} \sum_{j \in \underline{M}} \left[f(\varsigma_+^{j+1}/\varsigma_+^j) - f(\varsigma_+^j/\varsigma_-^j) \right] > 0. \end{aligned}$$

As a result, $\delta \phi_i \rightarrow 2\pi/n$ for all i as $t \rightarrow \infty$.

The circular formation is “almost globally” stable because there is a measure-zero set characterized by those configurations that two or more robots have same ϕ_i . However, these equilibria are unstable. \square

4. Experiments

An experimental platform that contains a team of e-puck robot is developed in our laboratory for demonstrating the effectiveness of the proposed control schemes. Because the sensing capability of the e-puck robot is very limited, in the current implementation, bearing measurements are provided by a central computer through a calibrated overhead camera. Color triangular marks are placed on the top of each robot. These marks are identified by the camera for tracking robot pose. However, only relative bearing information are utilized in order to mimic local and distributed implementation of the proposed control schemes. Although this is not a real distributed implementation, it still provides us a platform to test the performance of the proposed controllers under many practical issues, such as unmodeled dynamics and errors, noise, delays caused by sensing and information processing, and also the switching of controllers to avoid collision with others robots and boundaries which is not accounted in the theoretical analysis.

4.1. Collision avoidance

In the theoretical analysis, the robots are treated as moving points. However, a real robot is never a point, and therefore collision avoidance cannot be negligible when several robots work together in a region. Collision avoidance itself, especially for nonholonomic mobile robots, is a challenging problem (see Kan, Dani, Shea, & Dixon, 2012, Mastellone, Stipanović, Graunke, Intlekofer, & Spong, 2008 and references therein). Designing a totally distributed and mathematically provable bearing-only collision avoidance algorithm remains an unsolved problem and we are still working on it. In our experiments, a behavior-based algorithm is adopted, which is straightforward and computationally effective.

It should be pointed out that the current collision avoidance scheme uses not only bearing information. We need to assume that within a certain sensing zone $Q^i := \{j | \sqrt{(x_j - x_i)^2 + (y_j - y_i)^2} \leq d_s, j \neq i\}$, a robot can detect both the bearing and range information about other robots (see Fig. 4). This can be done, for example, by using short-range infra-red proximity sensors mounted on the body of the mobile robot. The forward speeds v_i are multiplied by a variable m_i and become $\tilde{v}_i = m_i v_i$, where

Table 1
Parameters used in experiments.

v_{\max}	ω_{\max}	ρ^*	r_s	d_s	d_c
6 cm/s	2.43 rad/s	24 cm	40 cm	15 cm	9 cm

$$m_i = \begin{cases} 1, & \text{if } Q^i = \emptyset, \\ 0, & \text{if } Q_1^i \neq \emptyset, \\ 0, & \text{if } Q_2^i \neq \emptyset \text{ and } |v_i| < |v_j|, \exists j \in Q_2^i, \\ 2, & \text{if } Q_1^i = \emptyset, Q_2^i \neq \emptyset \text{ and } |v_i| > |v_j|, \forall j \in Q_2^i, \\ 2, & \text{if } Q_1^i = \emptyset, Q_2^i = \emptyset, \text{ and } Q_3^i \neq \emptyset. \end{cases}$$

The partitions Q_1^i , Q_2^i , and Q_3^i are formally defined as

$$Q_1^i := \{j | x_j^i \cdot v_i \geq 0 \wedge |y_j^i| \leq d_c\} \cap Q^i,$$

$$Q_2^i := \{j | x_j^i \cdot v_i \geq 0 \wedge |y_j^i| > d_c\} \cap Q^i,$$

$$Q_3^i := \{j | x_j^i \cdot v_i < 0\} \cap Q^i.$$

Notice that \tilde{v}_i may not be achieved due to saturation of the actuator. This collision avoidance algorithm was found to work well in the experiment. One of the reasons is that the proposed controllers themselves tend to separate the robots from each other.

Since the working area is bounded, the robots should also avoid collision with the boundaries and keep inside the working area. To do that, on detecting the boundaries, a robot stops moving forward and rotates at the maximal angular speed for a short time span until its forward direction (the direction of v_i) points into the bounded area again.

4.2. Experimental results

Due to space limitation, only the experimental results for the multirobot case are shown here. We performed tests of enclosing a target with five e-puck robots. The parameters used in the experiments are given in Table 1.

We firstly applied the controller 4. Fig. 5(a) illustrates top-view snapshots from the actual trial, which are captured by the overhead camera. We set the coordination function to be $f(\sigma_+^i/\sigma_-^i) = 1 - \exp(-\sigma_+^i/\sigma_-^i)$. To test the performance of controller 4, the robots were placed at different locations with different orientations initially within the working area (see Fig. 5(a)). Figs. 5(b) and (c) illustrate the changes of $\rho_i(t) - \rho^*$ and $\sin[\phi_i + 2(i-1)\pi/n]$, respectively. One can observe that the five robots converged to the desired circle and achieved even distribution over the circle as expected. It is also pointed out here that the collision avoidance scheme does not affect the locally asymptotical stability result in Theorem 5, because at the equilibrium point all robots are in the same operational state, i.e., $m_i = m_j$ for any i and j , where $i \neq j$.

We then tested the performance of controller 5. We set $L = 3$ cm, $\beta^* = 0.8$ rad, $a = 1/2$ and let the function $f(\varsigma_+^i/\varsigma_-^i)$ in (22) be $1 - \exp(-\varsigma_+^i/\varsigma_-^i)$. To meet the requirement $\sqrt{k_\rho^2 + k_\phi^2} \leq \min(v_{\max}, \omega_{\max}|L|)$, k_ρ and k_ϕ should be small. However, small k_ρ and k_ϕ will lead to slow convergence. In the actual experiment, we set both k_ρ and k_ϕ to be 10. Satisfying results were obtained as shown in Figs. 6(a)–(c).

5. Conclusions

In this paper, the problem of enclosing a target by a single robot and multiple cooperative robots is investigated. We develop novel control schemes based on the local bearing measurements only, which are commonly available by using monocular vision systems. No communication is needed amongst the robots when using the proposed control schemes. We develop controller for single robot circumnavigation first, and then extend them to deal with the multirobot case. Using Lyapunov stability criteria, it has

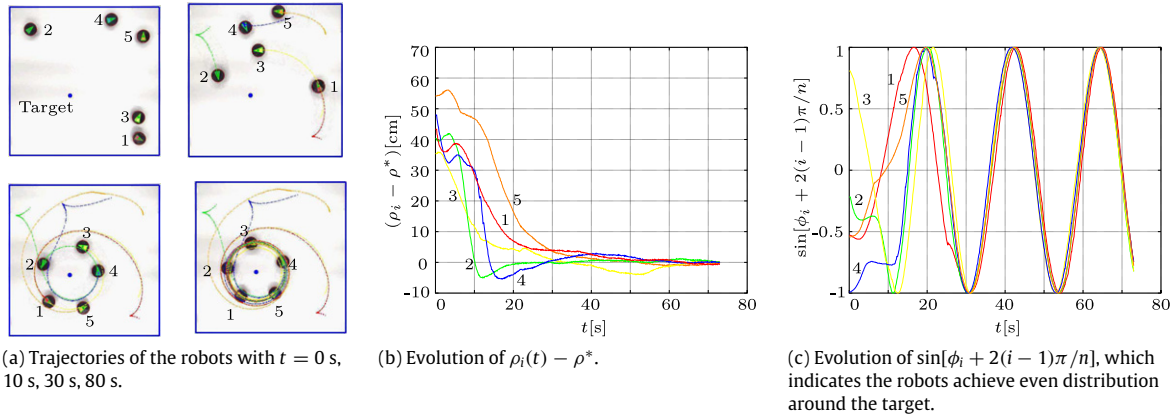


Fig. 5. Experimental result of controller 4.

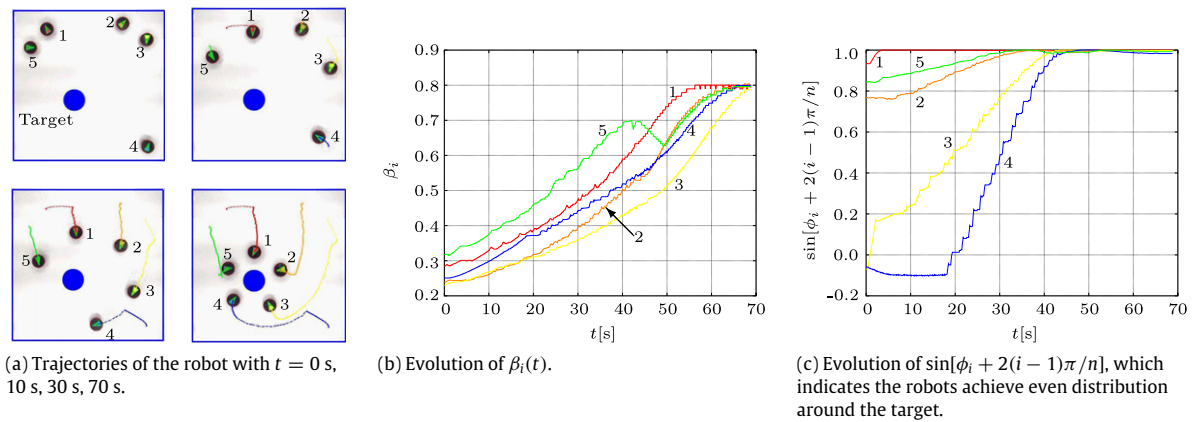


Fig. 6. Experimental result of controller 5.

been shown that the proposed control schemes can guarantee asymptotic convergence to the desired stand-off orbit despite the lack of direct metric information. In addition, a static circular formation control based on feedback linearization is studied. The experiment on a group of two-wheeled differential drive robots supports the effectiveness of the proposed control design.

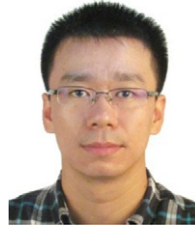
As part of our future work, we plan to implement the proposed control schemes in more dynamic environments and multi-target scenarios. In this paper, the robots use the measured subtended angle to avoid collision with disk targets. As a future research topic, we will consider inter-robot collision avoidance by using the subtended angle measurement without range measurement. This approach allows us to treat target enclosing and collision avoidance at the same time, which is very useful when the dynamics of the mobile robots is considered and the smoothness of the controllers becomes important. We also intend to implement the proposed control schemes on mobile robots which have the capability to directly measure the relative bearing information, such as those used in Chen, Sun, Yang, and Chen (2009), Li, Sun, and Yang (2013) and Sun, Wang, Shang, and Feng (2009).

References

- Basiri, M., Bishop, A., & Jensfelt, P. (2010). Distributed control of triangular formations with angle-only constraints. *Systems & Control Letters*, 59(2), 147–154.
- Bhat, S., & Bernstein, D. (1997). Finite-time stability of homogeneous systems. In *Proceedings of the 1997 American nuclear conference*, Vol. 4 (pp. 2513–2514).
- Bishop, A. (2011a). A very relaxed control law for bearing-only triangular formation control. In *Proceedings of 2011 IFAC world congress* (pp. 5991–5998).

- Bishop, A. (2011b). Distributed bearing-only quadrilateral formation control. In *Proceedings of 2011 IFAC world congress*.
- Bishop, A., Fidan, B., Anderson, B., Doğançay, K., & Pathirana, P. (2010). Optimality analysis of sensor-target localization geometries. *Automatica*, 46(3), 479–492.
- Bishop, A., Shames, I., & Anderson, B. (2011). Stabilization of rigid formations with direction-only constraints. In *Proceedings of 2011 IEEE conference on decision and control and European control conference* (pp. 746–752). IEEE.
- Cao, Y., Muse, J., Casbeer, D., & Kingston, D. (2013). Circumnavigation of an unknown target using uavs with range and range rate measurements. *ArXiv Preprint arXiv:1308.6250*.
- Ceccarelli, N., Di Marco, M., Garulli, A., & Giannitrapani, A. (2008). Collective circular motion of multi-vehicle systems. *Automatica*, 44(12), 3025–3035.
- Chen, J., Sun, D., Yang, J., & Chen, H. (2009). A leader-follower formation control of multiple nonholonomic mobile robots incorporating receding-horizon scheme. *The International Journal of Robotics Research*, 29(6), 727–747.
- Deghat, M., Davis, E., See, T., Shames, I., Anderson, B., & Yu, C. (2012). Target localization and circumnavigation by a non-holonomic robot. In *Proceedings of 2012 IEEE/RSJ international conference on intelligent robots and systems* (pp. 1227–1232). IEEE.
- Deghat, M., Shames, I., Anderson, B., & Yu, C. (2010). Target localization and circumnavigation using bearing measurements in 2D. In *Proceedings of 49th IEEE conference on decision and control* (pp. 334–339).
- Eren, T. (2012). Formation shape control based on bearing rigidity. *International Journal of Control*, 85(9), 1361–1379.
- Feddema, J., Lewis, C., & Schoenwald, D. (2002). Decentralized control of cooperative robotic vehicles: theory and application. *IEEE Transactions on Robotics and Automation*, 18(5), 852–864.
- Franchi, A., Masone, C., Grabe, V., Ryll, M., Bühlhoff, H., & Giordano, P. (2012). Modeling and control of uav bearing formations with bilateral high-level steering. *The International Journal of Robotics Research*, 31(12), 1504–1525.
- Guo, J., Yan, G., & Lin, Z. (2010). Local control strategy for moving-target-enclosing under dynamically changing network topology. *Systems & Control Letters*, 59(10), 654–661.
- Guo, J., Yan, G., & Lin, Z. (2011). Balanced circular formation control based on gossip communication and angle of arrival information. In *Proceedings of the 2011 Chinese control conference* (pp. 6036–6041).
- Kan, Z., Dani, A., Shea, J. M., & Dixon, W. E. (2012). Network connectivity preserving formation stabilization and obstacle avoidance via a decentralized controller. *IEEE Transactions on Automatic Control*, 57(7), 1827–1832.

- Khalil, H. (2002). *Nonlinear systems* (3rd ed.). Prentice Hall.
- Kim, T., & Sugie, T. (2007). Cooperative control for target-capturing task based on a cyclic pursuit strategy. *Automatica*, 43(8), 1426–1431.
- Lan, Y., Yan, G., & Lin, Z. (2010). Distributed control of cooperative target enclosing based on reachability and invariance analysis. *Systems & Control Letters*, 59(7), 381–389.
- Lawton, J., Beard, R., & Young, B. (2003). A decentralized approach to formation maneuvers. *IEEE Transactions on Robotics and Automation*, 19(6).
- Li, X., Sun, D., & Yang, J. (2013). A bounded controller for multirobot navigation while maintaining network connectivity in the presence of obstacles. *Automatica*, 49(1), 285–292.
- Mastellone, S., Stipanović, D., Graunke, C., Intlekofer, K. A., & Spong, M. (2008). Formation control and collision avoidance for multi-agent non-holonomic systems: theory and experiments. *The International Journal of Robotics Research*, 27(1), 107–126.
- Matveev, A., Høy, M., & Savkin, A. (2013). A method for reactive navigation of nonholonomic under-actuated robots in maze-like environments. *Automatica*, 49(5), 1268–1274.
- Moshtaghi, N., Michael, N., Jadbabaie, A., & Daniilidis, K. (2009). Vision-based, distributed control laws for motion coordination of nonholonomic robots. *IEEE Transactions on Robotics*, 25(4), 851–860.
- Shames, I., Dasgupta, S., Fidan, B., & Anderson, B. (2012). Circumnavigation using distance measurements under slow drift. *IEEE Transactions on Automatic Control*, 57(4), 889–903.
- Sun, D., Wang, C., Shang, W., & Feng, G. (2009). A synchronization approach to trajectory tracking of multiple mobile robots while maintaining time-varying formations. *IEEE Transactions on Robotics*, 25(5), 1074–1086.
- Tang, S., Shinzaki, D., Gage, C.G., & Clark, C. (2012). Multi-robot control for circumnavigation of particle distributions. In *11th International symposium on distributed autonomous robotic systems*.
- Yamaguchi, H. (1999). A cooperative hunting behavior by mobile-robot troops. *The International Journal of Robotics Research*, 18(9), 931–940.
- Zhao, S., Lin, F., Peng, K., Chen, B., & Lee, T. (2013). Finite-time stabilisation of cyclic formations using bearing-only measurements. *International Journal of Control*, 1–13 (ahead-of-print).
- Zheng, R., Lin, Z., Fu, M., & Sun, D. (2013). Distributed circumnavigation by unicycles with cyclic repelling strategies. In *Proceedings of 9th Asian control conference*.
- Zheng, R., & Sun, D. (2013a). Rendezvous of unicycles: a bearings-only and perimeter shortening approach. *Systems & Control Letters*, 62(5), 401–407.
- Zheng, R., & Sun, D. (2013b). Rendezvous of wheeled mobile robots using bearings-only or range-only measurements. In *Proceedings of IEEE international conference on robotics and biomimetics*.



Ronghao Zheng received his Bachelor degree in Electrical Engineering and master degree in Control Theory and Control Engineering both from Zhejiang University, China in 2007 and 2010, respectively. He received his Ph.D. degree from the Department of Mechanical and Biomedical Engineering, City University of Hong Kong in 2014. He is currently with the Department of Systems Science and Engineering, Zhejiang University, China. His research interests lie in the area of distributed algorithms and control, particularly the coordination of networked mobile robot teams with applications in automated systems and security.



Yunhui Liu received his B.Eng. degree in Applied Dynamics from Beijing Institute of Technology, China, in 1985, his M.Eng. degree in Mechanical Engineering from Osaka University in 1989, and his Ph.D. degree in Mathematical Engineering and Information Physics from the University of Tokyo, Japan, in 1992. He worked at the Electrotechnical Laboratory, MITI, Japan from 1992 to 1995 as a Research Scientist. He has been with Department of Mechanical and Automation Engineering, The Chinese University of Hong Kong since 1995, and is currently a Professor, Director of Networked Sensors and Robotics Laboratory, Director of Medical Robotics Laboratory, and Director of Centre for Robotics and Technology Education. Professor Liu is interested in medical robotics, vision-based robot control, aerial robotics, multi-fingered grasping, networked robotics, and robot applications. He is the Editor-in-Chief of Robotics and Biomimetics and an Editor of Advanced Robotics, and was an Associate Editor of IEEE Transactions on Robotics and Automation. He is a Fellow of IEEE.



Dong Sun is currently a Chair professor and Head of the Department of Mechanical and Biomedical Engineering, City University of Hong Kong. He received the Bachelor and Master's degrees from Tsinghua University, Beijing, China, and the Ph.D. degree in robotics and automation from the Chinese University of Hong Kong, Hong Kong, China. He then was a Postdoctoral researcher at the University of Toronto, Canada, and a Research and Development Engineer in Ontario industry. Prof. Sun has particular research interests in robot control and robot-aided cell manipulation in recent years. He has served on the editorial boards for many international journals including IEEE Transactions on Robotics and IEEE/ASME Transactions on Mechatronics. He is a Fellow of IEEE.